

Parametric Study on RPV Integrity Assessment under Pressurized Thermal Shock

***Jongwook Kim¹, Hanbum Surh¹, and Shinbeom Choi¹**

¹Korea Atomic Energy Research Institute, Republic of Korea

*Presenting & Corresponding author: kjwook1231@gmail.com

Abstract

The objective of this study is to evaluate the structural integrity of a reactor pressure vessel during a pressurized thermal shock event by applying deterministic fracture mechanics. The deterministic fracture mechanics analysis was performed using three-dimensional finite element models. The impacts of the input parameters, such as the crack location, the aspect ratio, and the cladding properties were reviewed through the corresponding sensitivity analyses. In addition, the maximum allowable transition temperatures were estimated.

Keywords: Reactor Pressure vessel (RPV), Pressurized Thermal Shock, Deterministic Fracture Mechanics

Introduction

The reactor pressure vessel integrity is ensured by a proper margin between its loads bearing capacity given by the vessel design and material properties, and the acting loads, which could occur during a plant operation. Thus, it is designed and manufactured according to the strict code requirements to ensure its structural integrity.

Before the late 1970s, it was postulated that the most severe thermal shock that a pressurized water reactor (PWR) vessel must withstand is a large break loss of coolant accident (LOCA). In this type of overcooling transient, low-temperature emergency core coolant will rapidly enter the reactor pressure vessel (RPV) and cool the vessel wall. The resulting temperature gradient in the vessel wall will cause a significant thermal stress, within the inner surface of the wall. However, the stresses due to the system pressure along with the thermal stresses were not considered, since it was expected that during a large break LOCA, the system will depressurize fast and remain at a low pressure. In 1978, the occurrence of a pressurized thermal shock (PTS) at the Rancho Seco nuclear power plant in California showed that some overcooling transients can be accompanied by a re-pressurization of the primary system, which will compound the effects of the thermal stresses. When a system pressure remains high or slowly decreases during thermal shock events, an additional stress from the system pressure greatly increases the possibility of a crack initiation and propagation. In particular, the surface cracks and underclad cracks located in the RPV inner wall can pose concerns under a PTS event. To assure the integrity of RPVs under a PTS event, the PTS rule requires that the RT_{NDT} of RPV beltline materials should be lower than the PTS screening criteria. However, a PTS analysis for the integrity of a RPV is a complex task, which places significant requirements on the experts performing it. These requirements include knowledge of the dominant physical phenomena and associated computer codes, knowledge of the plant being analyzed, and knowledge of the relevant codes and standards for a RPV integrity assessment. In addition, several different procedures and approaches are presently used for the integrity assessments of RPVs. This implies that the results from the assessments are not comparable between individual RPVs as different procedures and approaches are used.

Therefore, it is necessary to undertake a parameter study for the fracture mechanics evaluation of a RPV under a PTS event.

The objective of this study is to evaluate the structural integrity of a RPV under PTS conditions by applying deterministic fracture mechanics. The deterministic fracture mechanics analysis was performed using three-dimensional finite element models. The crack configurations, crack aspect ratio, and cladding properties were considered in the parametric study. In addition, the maximum allowable transition temperatures were investigated.

Problem Definition

Geometric

The RPV considered in the analysis is a typical 3-loop PWR, which is made of ASTM A508 Class 3 with an inner radius of 1994 mm, a base metal thickness of 200 mm, and a cladding thickness of 7.5 mm. The postulated defect as a base case (Case 1) is a through-clad surface-breaking semi-elliptical crack of 19.5 mm in depth by 117 mm in length for $a/c = 1/3$, as shown in Fig. 1. The configuration of an elliptical underclad crack (Case 6) is shown in Fig. 2.

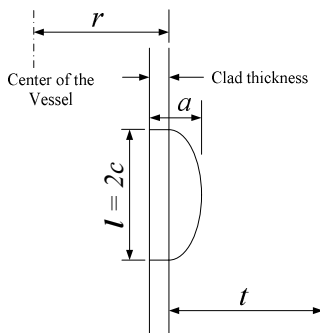


Figure 1. Schematic Illustration of a postulated crack (Case 1)

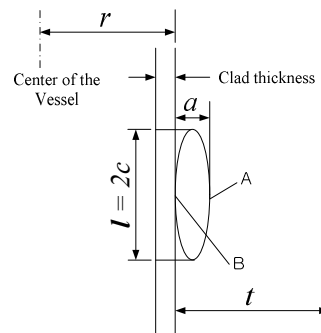


Figure 2. Schematic Illustration of a postulated crack (Case 6)

Transient Conditions

One overcooling transient due to an assumed leak is defined as in Fig. 3, for which axisymmetric loading conditions are assumed. The figure shows a typical PTS transient with repressurization. The temperature and pressure start to decrease, but at a certain time, namely, about 7200 seconds after the transient begins, the system pressure increases rapidly. It is maintained and a slow heating occurs, which shows the typical characteristics of a PTS transient. In this case, the pressure is assumed to be a dominant factor.

Sensitivity Study

Several parametric studies are proposed to investigate the influence of certain parameters on the results. Of them, considered here is a postulated defect of those parameters such as underclad vs. surface cracking, defect aspect ratio ($a/c=1/3, 1/2, 1/1$), and elliptical vs. semielliptical cracking. An analysis matrix for the sensitivity of the postulated defect is shown in Table 1. In addition, the effects of the cladding are investigated for three conditions of Case 1 as follows:

- C1: No cladding. Cladding properties are assumed as identical to the base metal.
- C2: Cladding thermal conductivity is considered. Additional stress due to a steep temperature gradient in the cladding is evaluated.
- C3: Cladding is fully considered. Additional stresses due to a steep temperature gradient and a differential thermal expansion are evaluated.

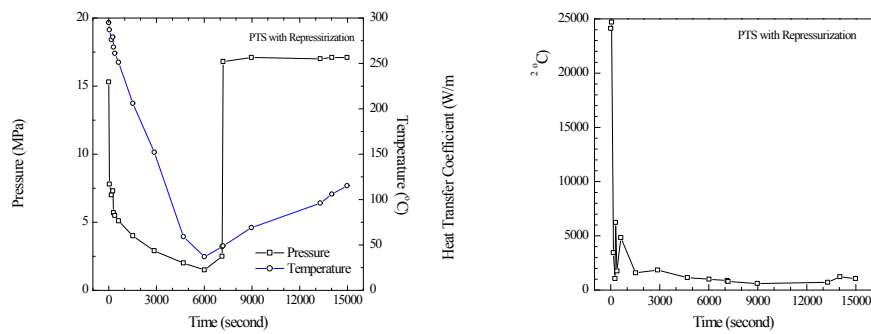


Figure 3. Transient histories of a PTS with repressurization

Table 1. Analysis matrix for a sensitivity study of a postulated defect

Case	Location	Shape	Aspect ratio (a/c)	Depth	
				a	a/t
1	surface	semi-elliptical	1/3	19.5	0.06
2	underclad	semi-elliptical	1/3	12.0	0.06
3	underclad	semi-elliptical	1/3	15.0	0.075
4	surface	semi-elliptical	1/2	19.5	0.06
5	surface	semi-elliptical	1/1	19.5	0.06
6	underclad	elliptical	1/3	12.0	0.06

Finite Element Modeling

In this paper, three-dimensional finite element analyses were performed for an assessment of various cracks in the RPV under PTS conditions. The model was designed using 20-node isoparametric quadratic brick elements with reduced Gaussian integration points and 20-node quarter point brick elements for the crack front point. Typical examples of the meshes are shown in Figs. 4 (semi-elliptical surface crack) and 5 (elliptical underclad crack), respectively. Three-dimensional finite element analyses, including thermal and mechanical calculations, were performed using the ABAQUS finite element analysis program. For each geometrical configuration, the stress intensity factor was calculated from the value of the J-integral obtained at the deepest point.

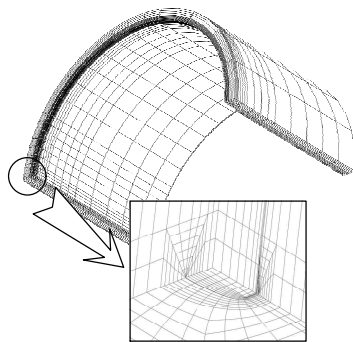


Figure 4. 3-Dimensional FE mesh for the semi-elliptical surface crack

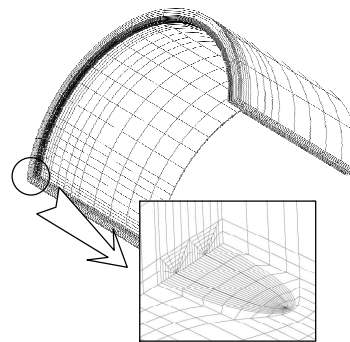


Figure 5. 3-Dimensional FE mesh for the elliptical underclad crack

Finite Element Analysis Results

Maximum Allowable RT_{NDT}

The maximum allowable nil ductile transition temperature for each crack geometric under a PTS event is presented in Table 2.

Effects of Crack Aspect Ratio

The effects of the crack aspect ratio on the stress intensity factor curves are shown in Fig. 6. The stress intensity factor curves decrease with an increase in the crack aspect ratio.

Influence of Crack Configuration

The effects of the crack location are shown in Fig. 7 for surface and underclad cracking. The stress intensity factor for a surface crack is much higher than that of an underclad crack with the same deepest point. In Case 2_C3, the stress intensity factor is so small that crack initiation does not occur during the transient event. Fig. 8 shows the stress intensity factor curves for the existing cracks in the base metal. The two results show a similar tendency. The stress intensity factor curves at two crack tip points are shown in Fig. 9 for the elliptical underclad crack. The stress intensity factor curve at point B is much higher than that of point A at the deepest point of a crack front. This means that it is possible to predict a crack initiation at point B.

Influence of Cladding Properties

Fig. 10 shows the stress intensity factor curves with different properties of the cladding. The curve of Case 1_C3 is much higher than that of Cases 1_C2 and C3. Accordingly, the maximum allowable RT_{NDT} of Case 1_C3 is the lowest.

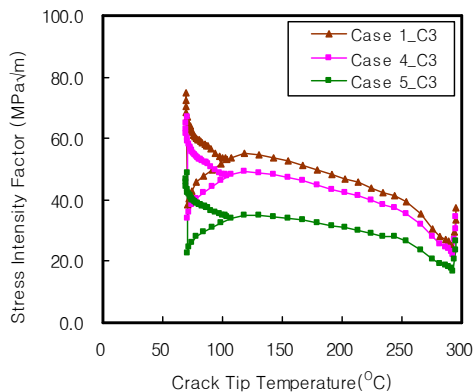


Figure 6. Comparison of the SIF with various crack aspect ratios

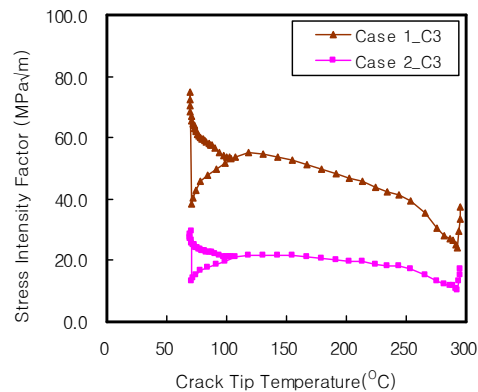


Figure 7. Comparison of the SIF with various crack locations

Conclusions

In this paper, three-dimensional finite element analyses were performed to evaluate the integrity of a RPV under PTS conditions, and the following conclusions were obtained.

1. Stress discontinuity takes place at a boundary line between the cladding and base metal.
2. As the crack aspect ratio increases with the same crack depth, the maximum allowable nil ductile transition temperature increases.

3. When the differences in the thermal conductivity and the thermal expansion coefficients of a cladding are fully considered, the stress intensity factor curve increases.
4. The stress intensity factor of a surface crack is much higher than that of an underclad crack with the same deepest point.
5. For an elliptical underclad crack, the possibility of a crack initiation was monitored at the boundary between the cladding and base metal.

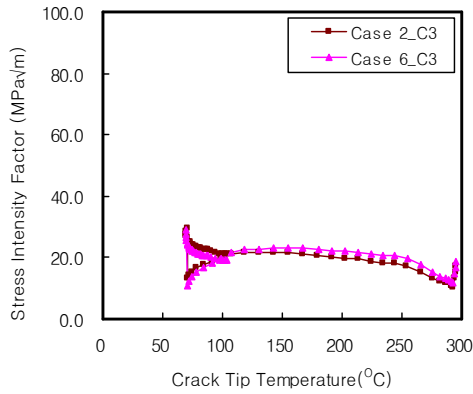


Figure 8. Comparison of the SIF with various crack shapes

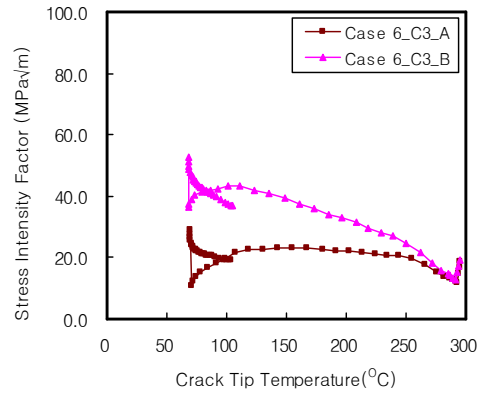


Figure 9. Comparison of the SIF with crack tip points

Table 2. Maximum Allowable RT_{NDT} by the maximum criteria at the deepest point

Case	Cladding	Maximum allowable RT_{NDT} (°C)
1	C1	69
	C2	71
	C3	56
2	C3	No intersection
3	C3	62
4	C3	No intersection
5	C3	89
6	C3 (Point A)	No intersection
	C3 (Point B)	78

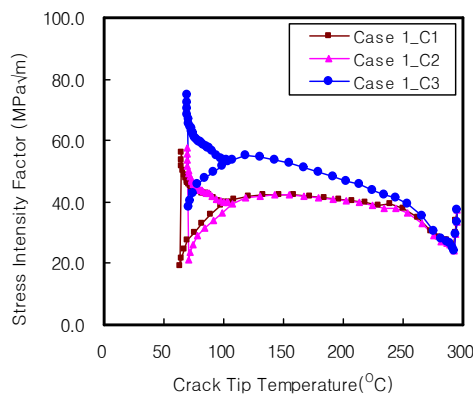


Figure 10. Comparison of the SIF with various thermal/mechanical properties of the cladding

Acknowledgement

This work was supported by the National Research Foundation of Korea (NRF) grant funded by the Korea government (MSIT) (2016M2C6A1930040).

References

- [1] U.S. Nuclear Regulatory Commission (1997): “Fracture toughness requirements for protection against pressurized thermal shock events”, 10 CFR 50.61.
- [2] The American Society of Mechanical Engineers (2007): “Protection against nonductile failure”, ASME Boiler and Pressure Vessel Code Section III, Appendix G.
- [3] The American Society of Mechanical Engineers (2007): “Rules for inservice inspection of nuclear power plant components”, ASME Boiler and Pressure Vessel Code Section XI, Appendix A.